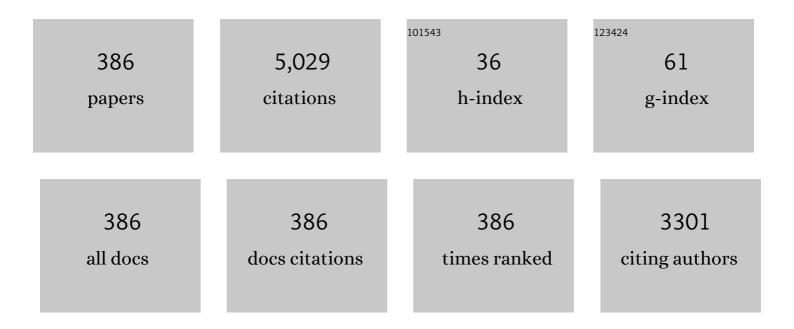
## **Tomas Mocek**

List of Publications by Year in descending order

Source: https://exaly.com/author-pdf/6973157/publications.pdf Version: 2024-02-01



#	Article	IF	CITATIONS
1	A high-intensity highly coherent soft X-ray femtosecond laser seeded by a high harmonic beam. Nature, 2004, 431, 426-429.	27.8	313
2	The Prague Asterix Laser System. Physics of Plasmas, 2001, 8, 2495-2501.	1.9	259
3	High-speed manufacturing of highly regular femtosecond laser-induced periodic surface structures: physical origin of regularity. Scientific Reports, 2017, 7, 8485.	3.3	251
4	Laser-Driven Proton Acceleration Enhancement by Nanostructured Foils. Physical Review Letters, 2012, 109, 234801.	7.8	178
5	Kilowatt average power 100  J-level diode pumped solid state laser. Optica, 2017, 4, 438.	9.3	152
6	Multimillijoule, highly coherent x-ray laser at 21 nm operating in deep saturation through double-pass amplification. Physical Review A, 2002, 66, .	2.5	110
7	Ultrashort pulse laser ablation of dielectrics: Thresholds, mechanisms, role of breakdown. Scientific Reports, 2016, 6, 39133.	3.3	110
8	Generation of submicrojoule high harmonics using a long gas jet in a two-color laser field. Applied Physics Letters, 2008, 92, .	3.3	106
9	Demonstration of a Ni-Like Kr Optical-Field-Ionization Collisional Soft X-Ray Laser at 32.8Ânm. Physical Review Letters, 2002, 89, 253901.	7.8	91
10	Verdet Constant of Magneto-Active Materials Developed for High-Power Faraday Devices. Applied Sciences (Switzerland), 2019, 9, 3160.	2.5	77
11	Demonstration of a Collisionally Excited Optical-Field-Ionization XUV Laser Driven in a Plasma Waveguide. Physical Review Letters, 2003, 91, 205001.	7.8	74
12	100  J-level nanosecond pulsed diode pumped solid state laser. Optics Letters, 2016, 41, 2089.	3.3	73
13	Relaxation dynamics of femtosecond-laser-induced temperature modulation on the surfaces of metals and semiconductors. Applied Surface Science, 2016, 374, 157-164.	6.1	72
14	Spectroscopic characterization of Yb3+-doped laser materials at cryogenic temperatures. Applied Physics B: Lasers and Optics, 2014, 116, 75-81.	2.2	70
15	Full characterization of laser-accelerated ion beams using Faraday cup, silicon carbide, and single-crystal diamond detectors. Journal of Applied Physics, 2011, 109, .	2.5	68
16	Status of the High Average Power Diode-Pumped Solid State Laser Development at HiLASE. Applied Sciences (Switzerland), 2015, 5, 637-665.	2.5	65
17	Temperature-wavelength dependence of terbium gallium garnet ceramics Verdet constant. Optical Materials Express, 2016, 6, 3683.	3.0	63
18	High-Contrast, High-Intensity Petawatt-Class Laser and Applications. IEEE Journal of Selected Topics in Quantum Electronics, 2015, 21, 232-249.	2.9	60

#	Article	IF	CITATIONS
19	Microchip Yb:CaLnAlO_4 lasers with up to 91% slope efficiency. Optics Letters, 2017, 42, 2431.	3.3	57
20	Mechanisms of high-regularity periodic structuring of silicon surface by sub-MHz repetition rate ultrashort laser pulses. Applied Physics Letters, 2016, 109, .	3.3	56
21	Ablation pressure scaling at short laser wavelength. Physical Review E, 2003, 68, 067403.	2.1	53
22	Non-fluorinated superhydrophobic Al7075 aerospace alloy by ps laser processing. Applied Surface Science, 2019, 493, 287-293.	6.1	53
23	LIPSS on thin metallic films: New insights from multiplicity of laser-excited electromagnetic modes and efficiency of metal oxidation. Applied Surface Science, 2019, 491, 650-658.	6.1	50
24	Optimization of Wavefront Distortions and Thermal-Stress Induced Birefringence in a Cryogenically-Cooled Multislab Laser Amplifier. IEEE Journal of Quantum Electronics, 2013, 49, 960-966.	1.9	46
25	Modeling of amplified spontaneous emission, heat deposition, and energy extraction in cryogenically cooled multislab Yb^3+:YAG laser amplifier for the HiLASE Project. Journal of the Optical Society of America B: Optical Physics, 2012, 29, 1270.	2.1	45
26	Suppression of nonlinear phonon relaxation in Yb:YAG thin disk via zero phonon line pumping. Optics Letters, 2014, 39, 4919.	3.3	44
27	Overview of the HiLASE project: high average power pulsed DPSSL systems for research and industry. High Power Laser Science and Engineering, 2014, 2, .	4.6	43
28	Laser-driven high-energy proton beam with homogeneous spatial profile from a nanosphere target. Physical Review Special Topics: Accelerators and Beams, 2015, 18, .	1.8	43
29	Wavelength dependence of magneto-optic properties of terbium gallium garnet ceramics. Optics Express, 2015, 23, 13641.	3.4	42
30	Advances in High-Power, Ultrashort Pulse DPSSL Technologies at HiLASE. Applied Sciences (Switzerland), 2017, 7, 1016.	2.5	42
31	Hugoniot Data for Carbon at Megabar Pressures. Physical Review Letters, 2004, 92, 065503.	7.8	41
32	Hydrophilic to ultrahydrophobic transition of Al 7075 by affordable ns fiber laser and vacuum processing. Applied Surface Science, 2020, 505, 144523.	6.1	41
33	Highly Efficient, Compact Tm3+:RE2O3 (RE = Y, Lu, Sc) Sesquioxide Lasers Based on Thermal Guiding. IEEE Journal of Selected Topics in Quantum Electronics, 2018, 24, 1-13.	2.9	40
34	Metal-like self-organization of periodic nanostructures on silicon and silicon carbide under femtosecond laser pulses. Journal of Applied Physics, 2013, 114, .	2.5	37
35	Characterization of the collisionally pumped optical-field-ionized soft-x-ray laser at41.8nmdriven in capillary tubes. Physical Review A, 2006, 73, .	2.5	36
36	Aberration-free laser beam in the soft x-ray range. Optics Letters, 2009, 34, 2438.	3.3	36

#	Article	IF	CITATIONS
37	Femtosecond 85  μm source based on intrapulse difference-frequency generation of 21  μm Letters, 2018, 43, 1335.	pulses. (	Optics
38	Pulsed laser modification of transparent dielectrics: what can be foreseen and predicted by numerical simulations?. Journal of the Optical Society of America B: Optical Physics, 2014, 31, C8.	2.1	35
39	How to optimize ultrashort pulse laser interaction with glass surfaces in cutting regimes?. Applied Surface Science, 2015, 336, 364-374.	6.1	35
40	Astrophysical radiative shocks: From modeling to laboratory experiments. Laser and Particle Beams, 2006, 24, 535-540.	1.0	34
41	Opacity Measurements of a Hot Iron Plasma Using an X-Ray Laser. Physical Review Letters, 2006, 97, 035001.	7.8	32
42	150 J DPSSL operating at 1.5 kW level. Optics Letters, 2021, 46, 5771.	3.3	32
43	lodine laser production of highly charged Ta ions. European Physical Journal D, 1996, 46, 1099-1115.	0.4	31
44	Investigation of Zn and Cu prepulse plasmas relevant to collisional excitation x-ray lasers. Physical Review A, 1997, 56, 4229-4241.	2.5	31
45	Absolute Time-Resolved X-Ray Laser Gain Measurement. Physical Review Letters, 2005, 95, 173902.	7.8	31
46	Spatio-temporal modification of femtosecond focal spot under tight focusing condition. Optics Express, 2015, 23, 11641.	3.4	31
47	Microchip laser operation of Yb-doped gallium garnets. Optical Materials Express, 2016, 6, 46.	3.0	31
48	Enhancement of soft x-ray emission from a cryogenically cooled Ar gas jet irradiated by 25 fs laser pulse. Applied Physics Letters, 2000, 76, 1819-1821.	3.3	30
49	Impacts of Ambient and Ablation Plasmas on Short- and Ultrashort-Pulse Laser Processing of Surfaces. Micromachines, 2014, 5, 1344-1372.	2.9	29
50	Periodic surface structures on titanium self-organized upon double femtosecond pulse exposures. Applied Surface Science, 2015, 336, 349-353.	6.1	29
51	Focusing a multimillijoule soft x-ray laser at 21nm. Applied Physics Letters, 2006, 89, 051501.	3.3	28
52	Faraday effect measurements of holmium oxide (Ho <sub>2</sub> O <sub>3</sub> ) ceramics-based magneto-optical materials. High Power Laser Science and Engineering, 2018, 6, .	4.6	28
53	Temperature-wavelength dependence of Verdet constant of Dy <sub>2</sub> O <sub>3</sub> ceramics. Optical Materials Express, 2019, 9, 2971.	3.0	28
54	Dramatic enhancement of xuv laser output using a multimode gas-filled capillary waveguide. Physical Review A, 2005, 71, .	2.5	26

#	Article	IF	CITATIONS
55	Picosecond green and deep ultraviolet pulses generated by a high-power 100  kHz thin-disk laser. Optics Letters, 2016, 41, 5210.	3.3	26
56	Spectroscopic investigations of thulium doped YAG and YAP crystals between 77â€ <sup>–</sup> K and 300â€ <sup>–</sup> K for short-wavelength infrared lasers. Journal of Luminescence, 2018, 202, 427-437.	3.1	26
57	Collimation of laser-produced plasmas using axial magnetic field. Laser and Particle Beams, 2015, 33, 175-182.	1.0	25
58	Optimization of beam quality and optical-to-optical efficiency of Yb:YAG thin-disk regenerative amplifier by pulsed pumping. Optics Letters, 2014, 39, 1441.	3.3	24
59	1-J operation of monolithic composite ceramics with Yb:YAG thin layers: multi-TRAM at 10-Hz repetition rate and prospects for 100-Hz operation. Optics Letters, 2015, 40, 855.	3.3	24
60	Laser-induced crystallization of anodic TiO <sub>2</sub> nanotube layers. RSC Advances, 2020, 10, 22137-22145.	3.6	23
61	Fourier-limited seeded soft x-ray laser pulse. Optics Letters, 2010, 35, 1326.	3.3	22
62	Extreme ultraviolet emission and confinement of tin plasmas in the presence of a magnetic field. Physics of Plasmas, 2014, 21, 053106.	1.9	22
63	Experimental study of radiative shocks at PALS facility. Laser and Particle Beams, 2010, 28, 253-261.	1.0	21
64	Lasing and thermal characteristics of Yb:YAG/YAG composite with atomic diffusion bonding. Laser Physics Letters, 2017, 14, 015001.	1.4	21
65	New observations on DUV radiation at 257â€nm and 206â€nm produced by a picosecond diode pumped thin-disk laser. Optics Express, 2019, 27, 24286.	3.4	21
66	Demonstration of a spatial filtering amplifier for high-order harmonics. Optics Letters, 2007, 32, 1498.	3.3	20
67	Design of high-energy-class cryogenically cooled Yb3+â^¶YAG multislab laser system with low wavefront distortion. Optical Engineering, 2013, 52, 064201.	1.0	20
68	Fabrication of functional superhydrophobic surfaces on carbon fibre reinforced plastics by IR and UV direct laser interference patterning. Applied Surface Science, 2020, 508, 144817.	6.1	20
69	Periodic Grating Structures on Metal Self-organized by Double-pulse Irradiation. Journal of Laser Micro Nanoengineering, 2014, 9, 234-237.	0.1	20
70	The effect of laser shock peening with and without protective coating on intergranular corrosion of sensitized AA5083. Corrosion Science, 2022, 194, 109925.	6.6	20
71	Laser-Ablation Rates Measured Using X-Ray Laser Transmission. Physical Review Letters, 2007, 99, 195002.	7.8	19
72	Spectroscopic and lasing characteristics of Yb:YGAG ceramic at cryogenic temperatures. Optical Materials Express, 2015, 5, 1289.	3.0	19

#	Article	IF	CITATIONS
73	Nanostructure fabrication on the top of laser-made micropillars for enhancement of water repellence of aluminium alloy. Materials Letters, 2019, 256, 126601.	2.6	19
74	Verdet constant of potassium terbium fluoride crystal as a function of wavelength and temperature. Optics Letters, 2020, 45, 1683.	3.3	19
75	Thomson parabola ion spectrograph with the microchannel plate image converter in investigations of highâ€Z laser plasma ion sources. Review of Scientific Instruments, 1996, 67, 1272-1274.	1.3	18
76	Shock pressure induced by 0.44 $\hat{l}$ $\!\!\!/4$ m laser radiation on aluminum targets. Laser and Particle Beams, 2003, 21, 481-487.	1.0	18
77	Observation of spectral gain narrowing in a high-order harmonic seeded soft-x-ray amplifier. Physical Review A, 2010, 81, .	2.5	18
78	Design and optimization of an adaptive optics system for a high-average-power multi-slab laser (HiLASE). Applied Optics, 2014, 53, 3255.	1.8	18
79	Faraday Rotation of Dy2O3, CeF3 and Y3Fe5O12 at the Mid-Infrared Wavelengths. Materials, 2020, 13, 5324.	2.9	18
80	Outline of the ELI-Beamlines facility. Proceedings of SPIE, 2011, , .	0.8	17
81	Picosecond thin-disk laser platform PERLA for multi-beam micromachining. OSA Continuum, 2021, 4, 940.	1.8	17
82	Measurements of the highest acceleration gradient for ions produced with a long laser pulse. Review of Scientific Instruments, 2010, 81, 02A506.	1.3	16
83	Effect of lateral radiative losses on radiative shock propagation. High Energy Density Physics, 2007, 3, 8-11.	1.5	15
84	Design of a kJ-class HiLASE laser as a driver for inertial fusion energy. High Power Laser Science and Engineering, 2014, 2, .	4.6	15
85	Graphene Q-Switched Compact Yb:YAG Laser. IEEE Photonics Journal, 2015, 7, 1-7.	2.0	15
86	Efficient laser performance of a cryogenic Yb:YAG laser pumped by fiber coupled 940 and 969 nm laser diodes. Laser Physics Letters, 2015, 12, 015002.	1.4	15
87	Verdet constant dispersion of CeF <sub>3</sub> in the visible and near-infrared spectral range. Optical Engineering, 2017, 56, 067105.	1.0	15
88	Investigations of collisionally pumped optical field ionization soft-x-ray lasers. Journal of the Optical Society of America B: Optical Physics, 2003, 20, 195.	2.1	14
89	Beam properties of a deeply saturated, half-cavity zinc soft-x-ray laser. Journal of the Optical Society of America B: Optical Physics, 2003, 20, 1386.	2.1	14
90	Single-shot soft x-ray laser-induced ablative microstructuring of organic polymer with demagnifying projection. Optics Letters, 2008, 33, 1087.	3.3	14

#	Article	IF	CITATIONS
91	Cryogenic Yb:YAG Laser Pumped by VBG-Stabilized Narrowband Laser Diode at 969 nm. IEEE Photonics Technology Letters, 2016, 28, 1328-1331.	2.5	14
92	Overview of ytterbium based transparent ceramics for diode pumped high energy solid-state lasers. High Power Laser Science and Engineering, 2018, 6, .	4.6	14
93	Micromachining of Invar with 784 Beams Using 1.3 ps Laser Source at 515 nm. Materials, 2020, 13, 2962.	2.9	14
94	Fatigue life enhancement of additive manufactured 316l stainless steel by LSP using a DPSS laser system. Surface Engineering, 2022, 38, 183-190.	2.2	14
95	Soft-x-ray emission from small-sized Ne clusters heated by intense, femtosecond laser pulses. Physical Review E, 2000, 62, 4461-4464.	2.1	13
96	Spectroscopic characterization of various Yb <sup>3+</sup> doped laser materials at cryogenic temperatures for the development of high energy class diode pumped solid state lasers. Proceedings of SPIE, 2013, , .	0.8	13
97	Large-Beam Picosecond Interference Patterning of Metallic Substrates. Materials, 2020, 13, 4676.	2.9	13
98	41.8â ^ nmXe8+laser driven in a plasma waveguide. Physical Review A, 2004, 70, .	2.5	12
99	Multi-millijoule, deeply saturated x-ray laser at 21.2 nm for applications in plasma physics. Plasma Physics and Controlled Fusion, 2002, 44, B207-B223.	2.1	11
100	Surface modification of organic polymer by dual action of extreme ultraviolet/visible-near infrared ultrashort pulses. Journal of Applied Physics, 2009, 105, 026105.	2.5	11
101	Filamented plasmas in laser ablation of solids. Plasma Physics and Controlled Fusion, 2009, 51, 035013.	2.1	11
102	Measuring the electron density gradients of dense plasmas by deflectometry using short-wavelength probe. Physics of Plasmas, 2010, 17, 122705.	1.9	11
103	Evolution of laser-produced Sn extreme ultraviolet source diameter for high-brightness source. Applied Physics Letters, 2014, 105, 074103.	3.3	11
104	Periodic nanostructures self-formed on silicon and silicon carbide by femtosecond laser irradiation. Applied Physics A: Materials Science and Processing, 2014, 117, 49-54.	2.3	11
105	Efficient ASE Management in Disk Laser Amplifiers With Variable Absorbing Clads. IEEE Journal of Quantum Electronics, 2014, 50, 1-9.	1.9	11
106	Comparative LIDT measurements of optical components for high-energy HiLASE lasers. High Power Laser Science and Engineering, 2016, 4, .	4.6	11
107	Performance comparison of Yb:YAG ceramics and crystal gain material in a large-area, high-energy, high average–power diode-pumped laser. Optics Express, 2020, 28, 3636.	3.4	11
108	Study of the stability of beam characteristics of the neon-like Zn X-ray laser using a half cavity. European Physical Journal D, 2003, 22, 31-40.	1.3	10

#	Article	IF	CITATIONS
109	Characterization of collisionally pumped optical-field-ionization soft X-ray lasers. Applied Physics B: Lasers and Optics, 2004, 78, 939-944.	2.2	10
110	25TW Ti:sapphire laser chain at PALS. Proceedings of SPIE, 2011, , .	0.8	10
111	Design of deformable mirrors for high power lasers. High Power Laser Science and Engineering, 2016, 4, .	4.6	10
112	Spectroscopy and diode-pumped continuous-wave laser operation of Tm:Y2O3 transparent ceramic at cryogenic temperatures. Applied Physics B: Lasers and Optics, 2020, 126, 1.	2.2	10
113	Experimental study on compression of 216-W laser pulses below 2  ps at 1030  nm with chirpec Bragg grating. Applied Optics, 2020, 59, 7938.	l yolume 1.8	10
114	Investigations of laser-induced damages in fused silica optics using x-ray laser interferometric microscopy. Journal of Applied Physics, 2010, 107, .	2.5	9
115	Amplification of picosecond pulses to 100 W by an Yb:YAG thin-disk with CVBG compressor. , 2015, , .		9
116	Crystal growth, low-temperature spectroscopy and multi-watt laser operation of Yb:Ca3NbGa3Si2O14. Journal of Luminescence, 2018, 197, 90-97.	3.1	9
117	Initiation of air ionization by ultrashort laser pulses: evidence for a role of metastable-state air molecules. Journal Physics D: Applied Physics, 2018, 51, 25LT02.	2.8	9
118	Anti-Reflection Nanostructures on Tempered Glass by Dynamic Beam Shaping. Micromachines, 2021, 12, 289.	2.9	9
119	Fs-laser-written erbium-doped double tungstate waveguide laser. Optics Express, 2018, 26, 30826.	3.4	9
120	X-ray microscopy of living multicellular organisms with the Prague Asterix lodine Laser System. Laser and Particle Beams, 2003, 21, 511-516.	1.0	8
121	Soft X-ray contact microscopy of nematode Caenorhabditis elegans. European Physical Journal D, 2004, 30, 235-241.	1.3	8
122	Effect of amplified spontaneous emission and parasitic oscillations on the performance of cryogenically-cooled slab amplifiers. Laser and Particle Beams, 2013, 31, 553-560.	1.0	8
123	Thermally induced depolarization in terbium gallium garnet ceramics rod with natural convection cooling. Journal of Optics (United Kingdom), 2015, 17, 065610.	2.2	8
124	Femtosecond Yb:YGAG ceramic slab regenerative amplifier. Optical Materials Express, 2018, 8, 615.	3.0	8
125	A high-brightness room temperature 2.7 <i>µ</i> m Er:Y <sub>2</sub> O <sub>3</sub> ceramic laser. Laser Physics Letters, 2019, 16, 035801.	1.4	8
126	Towards Rapid Fabrication of Superhydrophobic Surfaces by Multi-Beam Nanostructuring with 40,401 Beams. Nanomaterials, 2021, 11, 1987.	4.1	8

#	Article	IF	CITATIONS
127	Characterization of focused beam of desktop 10-Hz capillary-discharge 46.9-nm laser. Proceedings of SPIE, 2009, , .	0.8	8
128	Novel unstable resonator configuration for highly efficient cryogenically cooled Yb:YAG Q-switched laser. Optics Express, 2019, 27, 21622.	3.4	8
129	Laser performances of diode pumped Yb:Lu <sub>2</sub> O <sub>3</sub> transparent ceramic at cryogenic temperatures. Optical Materials Express, 2019, 9, 4669.	3.0	8
130	Progress in optical-field-ionization soft X-ray lasers at LOA. Laser and Particle Beams, 2005, 23, .	1.0	7
131	Second generation X-ray lasers. Journal of Quantitative Spectroscopy and Radiative Transfer, 2006, 99, 142-152.	2.3	7
132	Development and applications of multimillijoule softX-ray lasers. Journal of Modern Optics, 2007, 54, 2571-2583.	1.3	7
133	Enhanced surface structuring by ultrafast XUV/NIR dual action. New Journal of Physics, 2011, 13, 053049.	2.9	7
134	New methods for high current fast ion beam production by laser-driven acceleration. Review of Scientific Instruments, 2012, 83, 02B307.	1.3	7
135	HiLASE cryogenically-cooled diode-pumped laser prototype for inertial fusion energy. Proceedings of SPIE, 2013, , .	0.8	7
136	Joule-Class 940-nm Diode Laser Bars for Millisecond Pulse Applications. IEEE Photonics Technology Letters, 2015, 27, 1663-1666.	2.5	7
137	Ultrashort-pulse laser processing of transparent materials: insight from numerical and semi-analytical models. Proceedings of SPIE, 2016, , .	0.8	7
138	Laser-induced periodic surface structures formation: investigation of the effect of nonlinear absorption of laser energy in different materials. Proceedings of SPIE, 2017, , .	0.8	7
139	Efficient diode pumped Yb:Y2O3 cryogenic laser. Applied Physics B: Lasers and Optics, 2019, 125, 1.	2.2	7
140	Balancing the conversion efficiency and beam quality of second harmonic generation of a two-picosecond Yb:YAG thin-disk laser. Laser Physics, 2020, 30, 025405.	1.2	7
141	Diode-pumped, electro-optically <i>Q</i> -switched, cryogenic Tm:YAG laser operating at 1.88 μm. High Power Laser Science and Engineering, 2021, 9, .	4.6	7
142	<title>Investigation of soft x-ray emission in the water window for microscopy using a double-stream gas puff target irradiated with the Prague Asterix Laser System (PALS)</title> . , 2001, , .		6
143	Nanometric deformations of thin Nb layers under a strong electric field using soft x-ray laser interferometry. Journal of Applied Physics, 2005, 98, 044308.	2.5	6
144	Utilizing ablation of solids to characterize a focused soft X-ray laser beam. , 2007, , .		6

#	Article	IF	CITATIONS
145	Determination of the Ion Temperature in a Plasma Created by Optical Field Ionization. Contributions To Plasma Physics, 2007, 47, 352-359.	1.1	6
146	Plasma-based X-ray laser at 21Ânm for multidisciplinary applications. European Physical Journal D, 2009, 54, 439-444.	1.3	6
147	Simulation of performance of wavefront correction using deformable mirror in high-average-power laser systems. , 2013, , .		6
148	Short-wavelength ablation of polymers in the high-fluence regime. Physica Scripta, 2014, T161, 014066.	2.5	6
149	Cryogenically-cooled Yb:YGAG ceramic mode-locked laser. Optics Express, 2016, 24, 1402.	3.4	6
150	Efficient diode-pumped Er:KLu(WO_4)_2 laser at â^¼161  μm. Optics Letters, 2018, 43, 218.	3.3	6
151	Diode pumped cryogenic Yb:Lu3Al5O12 laser in continuous-wave and pulsed regime. Optics and Laser Technology, 2021, 135, 106720.	4.6	6
152	Spectroscopy and diode-pumped laser operation of transparent Tm:Lu <sub>3</sub> Al <sub>5</sub> O <sub>12</sub> ceramics produced by solid-state sintering. Optics Express, 2020, 28, 28399.	3.4	6
153	Choquet like sets in function spaces. Bulletin Des Sciences Mathematiques, 2003, 127, 397-437.	1.0	5
154	Homogeneous focusing with a transient soft X-ray laser for irradiation experiments. Optics Communications, 2006, 263, 98-104.	2.1	5
155	Measurements of opacity and temperature of warm dense matter heated by focused soft X-ray laser irradiation. High Energy Density Physics, 2009, 5, 110-113.	1.5	5
156	High-energy, picosecond regenerative thin-disk amplifier at 1 kHz. Proceedings of SPIE, 2012, , .	0.8	5
157	Progress in kW-class picosecond thin-disk lasers development at the HiLASE. Proceedings of SPIE, 2016, , $\cdot$	0.8	5
158	Numerical Analysis of Thermal Effects in a Concept of a Cryogenically Cooled Yb: YAG Multislab 10 J/100-Hz Laser Amplifier. IEEE Journal of Quantum Electronics, 2019, 55, 1-8.	1.9	5
159	Effect of Gd3+/Ga3+ on Yb3+ emission in mixed YAG at cryogenic temperature. Ceramics International, 2019, 45, 9418-9422.	4.8	5
160	Monoclinic zinc monotungstate Yb3+,Li+:ZnWO4: Part II. Polarized spectroscopy and laser operation. Journal of Luminescence, 2021, 231, 117811.	3.1	5
161	High Resolution X-Ray Laser Backlighting of Plasmas Using Spatial Filtering Technique. Springer Proceedings in Physics, 2009, , 417-425.	0.2	5
162	High power picosecond parametric mid-IR source tunable between 17 and 26  μm. Applied Optics, 2018 8412.	3, 57, 1.8	5

#	Article	IF	CITATIONS
163	Numerical analysis of beam distortion induced by thermal effects in chirped volume Bragg grating compressors for high-power lasers. Journal of the Optical Society of America B: Optical Physics, 2020, 37, 3874.	2.1	5
164	Investigation of the lasing performance of a crystalline-coated Yb:YAG thin-disk directly bonded onto a silicon carbide heatsink. Optics Express, 2022, 30, 7708.	3.4	5
165	High Pressure Laser-Generated Shocks and Application to EOS of Carbon. Journal of Physics: Conference Series, 2007, 71, 012001.	0.4	4
166	Experimental investigation of fast electron transport in solid density matter: Recent results from a new technique of X-ray energy-encoded 2D imaging. Laser and Particle Beams, 2009, 27, 643-649.	1.0	4
167	Ablative microstructuring with plasma-based XUV lasers and efficient processing of materials by dual action of XUV/NIR–VIS ultrashort pulses. Radiation Effects and Defects in Solids, 2010, 165, 551-558.	1.2	4
168	Precise curvature measurement of Yb:YAG thin disk. , 2015, , .		4
169	Time-resolved measurement of thermally induced aberrations in a cryogenically cooled Yb:YAG slab with a wavefront sensor. Applied Physics B: Lasers and Optics, 2016, 122, 1.	2.2	4
170	Diode pumped compact cryogenic Yb:YAG/Cr:YAG pulsed laser. Proceedings of SPIE, 2016, , .	0.8	4
171	How new laser development can help laser shock peening penetration to widen industrial applications?. , 2017, , .		4
172	Continuous-wave and passively Q-switched cryogenic Yb:KLu(WO_4)_2 laser. Optics Express, 2017, 25, 25886.	3.4	4
173	Diode-pumped master oscillator power amplifier system based on cryogenically cooled Tm:Y2O3 transparent ceramics. Optical Materials Express, 2021, 11, 1489.	3.0	4
174	<title>Collisional optical-field ionization soft x-ray lasers</title> ., 2001, 4505, 195.		3
175	Bessel spatial profile of a soft x-ray laser beam. Applied Physics Letters, 2010, 97, .	3.3	3
176	High-power, picosecond pulse thin-disk lasers in the Hilase project. Proceedings of SPIE, 2013, , .	0.8	3
177	Laser-induced ion acceleration at ultra-high laser intensities. Radiation Effects and Defects in Solids, 2015, 170, 271-277.	1.2	3
178	3-D Particle-in-Cell Simulation of Laser-Produced Plasma in Axial Magnetic Field. IEEE Transactions on Plasma Science, 2016, 44, 574-581.	1.3	3
179	Design of an Optimized Adaptive Optics System With a Photo-Controlled Deformable Mirror. IEEE Photonics Technology Letters, 2016, 28, 1422-1425.	2.5	3
180	A 100J-level nanosecond pulsed DPSSL for pumping high-efficiency, high-repetition rate PW-class lasers. Proceedings of SPIE, 2017, , .	0.8	3

#	Article	IF	CITATIONS
181	kW-class picosecond thin-disc prepulse laser Perla for efficient EUV generation. Journal of Micro/ Nanolithography, MEMS, and MOEMS, 2017, 16, 1.	0.9	3
182	Characteristics of a high-power picosecond mid-IR parametric generator/amplifier tunable between 1.5 and 3.2 $\hat{l}$ 4m. , 2019, , .		3
183	Characterization of Bivoj/DiPOLE 100: HiLASE 100-J/10-Hz diode pumped solid state laser. , 2018, , .		3
184	Tensor-to-matrix mapping in elasto-optics. Journal of the Optical Society of America B: Optical Physics, 2020, 37, 1090.	2.1	3
185	Investigation of soft X-ray emission from Ar clusters heated by ultrashort laser pulses. Laser and Particle Beams, 2002, 20, 51-57.	1.0	2
186	Advances in collisionally pumped optical-field-ionization soft x-ray lasers. , 2003, 5197, 119.		2
187	Laser driven shock experiments at PALS. European Physical Journal D, 2004, 54, C431-C443.	0.4	2
188	Advanced optical damage studies using x-ray laser interferometric microscopy. , 2005, , .		2
189	Beam properties of fully optimized, table-top, coherent source at 30 nm. Opto-electronics Review, 2011, 19, .	2.4	2
190	High energy density matter generation using a focused soft-X-ray laser for volumetric heating of thin foils. High Energy Density Physics, 2011, 7, 11-16.	1.5	2
191	Advanced LIDT testing station in the frame of the HiLASE Project. Proceedings of SPIE, 2012, , .	0.8	2
192	Comparative design study of 100 J cryogenically cooled Yb:YAG multi-slab amplifiers operating at 10 Hz. , 2012, , .		2
193	Performance of a 100J cryogenically cooled multi-slab amplifier with respect to the pump beam parameters and geometry. Proceedings of SPIE, 2012, , .	0.8	2
194	Evolution of β-SiC in laser-generated plasmas. Applied Surface Science, 2013, 272, 19-24.	6.1	2
195	In-situ optical phase distortion measurement of Yb:YAG thin disk in high average power regenerative amplifier. Proceedings of SPIE, 2013, , .	0.8	2
196	Experimental test of TOF diagnostics for PW class lasers. Proceedings of SPIE, 2013, , .	0.8	2
197	Enhanced TNSA acceleration with 0.1-1 PW lasers. Proceedings of SPIE, 2013, , .	0.8	2
198	Conceptual design of 100 J cryogenically-cooled multi-slab laser for fusion research. EPJ Web of Conferences, 2013, 59, 08004.	0.3	2

#	Article	IF	CITATIONS
199	Status of HiLASE project: High average power pulsed DPSSL systems for research and industry. EPJ Web of Conferences, 2013, 59, 08003.	0.3	2
200	50-mJ, 1-kHz Yb:YAG thin-disk regenerative amplifier with 969-nm pulsed pumping. , 2014, , .		2
201	Zero-phonon-line pumped 100-kHz Yb:YAG thin disk regenerative amplifier. Proceedings of SPIE, 2014, , .	0.8	2
202	EUV ablation: a study of the process. , 2015, , .		2
203	Temperature dependent absorption measurement of various transition metal doped laser materials. Proceedings of SPIE, 2015, , .	0.8	2
204	Wavelength tunability of laser based on Yb-doped YGAG ceramics. , 2015, , .		2
205	Commissioning of a kW-class nanosecond pulsed DPSSL operating at 105 J, 10 Hz. Proceedings of SPIE, 2017, , .	0.8	2
206	Passive Q switching of Yb:CNGS lasers by Cr <sup>4+</sup> :YAG and V <sup>3+</sup> :YAG saturable absorbers. Applied Optics, 2018, 57, 8236.	1.8	2
207	Generating 84 fs, 4 nJ directly from an Yb-doped fiber oscillator by optimization of the net dispersion. Laser Physics, 2019, 29, 065105.	1.2	2
208	Compact, diode-pumped, unstable cavity Yb:YAG laser and its application in laser shock peening. Optics Express, 2021, 29, 15724.	3.4	2
209	X-ray laser facility at the PALS centre. European Physical Journal Special Topics, 2001, 11, Pr2-589-Pr2-596.	0.2	2
210	Design of a 10 J, 100 Hz diode-pumped solid state laser. , 2019, , .		2
211	Multiple pulse nanosecond laser induced damage threshold on hybrid mirrors. , 2017, , .		2
212	Picosecond deep ultraviolet pulses generated by a 100 kHz thin-disk laser system. , 2019, , .		2
213	Numerical study of sum frequency ultrashort pulse compression in borate crystals. Journal of the Optical Society of America B: Optical Physics, 2020, 37, 3229.	2.1	2
214	Morphology of Meteorite Surfaces Ablated by High-Power Lasers: Review and Applications. Applied Sciences (Switzerland), 2022, 12, 4869.	2.5	2
215	Experimental investigation of line plasmas created by intensities 109- 1011Wcm-2. , 1996, , .		1
216	Statistical investigations of the beam stability of the double-pass amplified zinc soft X-ray laser at 21.2 nm. European Physical Journal D, 2003, 26, 59-65.	1.3	1

#	Article	IF	CITATIONS
217	Prague Asterix Laser System (PALS) - results and upgrades. , 2003, 5228, 651.		1
218	Observation of enhanced soft x-ray emission using nitrogen clusters ionized by intense, femtosecond laser. Journal of Applied Physics, 2003, 93, 3105-3107.	2.5	1
219	Progress on Collisionally Pumped Optical-Field-Ionization Soft X-Ray Lasers. IEEE Journal of Selected Topics in Quantum Electronics, 2004, 10, 1351-1362.	2.9	1
220	Development of soft x-ray lasers at PALS. , 2005, , .		1
221	Development of soft x-ray lasers at PALS and their applications in dense plasma physics. Proceedings of SPIE, 2007, , .	0.8	1
222	X-ray lasers as probes to measure plasma ablation rates. Proceedings of SPIE, 2007, , .	0.8	1
223	Laser-induced damage studies in optical elements using X-ray laser interferometric microscopy. Proceedings of SPIE, 2009, , .	0.8	1
224	Design and modeling of kW-class thin-disk lasers. Proceedings of SPIE, 2012, , .	0.8	1
225	Pilot experiment on proton acceleration using the 25 TW femtosecond Ti:Sapphire laser system at PALS. Nuclear Instruments and Methods in Physics Research, Section A: Accelerators, Spectrometers, Detectors and Associated Equipment, 2012, 690, 48-52.	1.6	1
226	Generation of periodic structures on SiC upon laser plasma XUV/NIR radiations. Laser and Particle Beams, 2013, 31, 547-550.	1.0	1
227	Zero-phonon-line pumped 1 kHz Yb:YAG thin-disk regenerative amplifier. , 2013, , .		1
228	Tunable mid-IR parametric conversion system pumped by a high-average-power picosecond Yb:YAG thin-disk laser. Proceedings of SPIE, 2014, , .	0.8	1
229	Active wavefront control in Hilase multislab high-average-power laser system. , 2014, , .		1
230	Characterization of diode-laser stacks for high-energy-class solid state lasers. Proceedings of SPIE, 2014, , .	0.8	1
231	High-energy picosecond light source based on cryogenically conduction cooled Yb-doped laser amplifier. Proceedings of SPIE, 2014, , .	0.8	1
232	Cooling options for high-average-power laser mirrors. , 2015, , .		1
233	Design and development of the HELL user station: beam transport, characterization, and shielding. , 2015, , .		1
234	Wavefront control in high average-power multi-slab laser system. , 2015, , .		1

1

#	Article	IF	CITATIONS
235	HiLASE: development of fully diode pumped disk lasers with high average power. , 2015, , .		1
236	Time-resolved deformation measurement of Yb:YAG thin disk using wavefront sensor. Proceedings of SPIE, 2015, , .	0.8	1
237	New possibilities for efficient laser surface treatment by diodeâ€pumped kWâ€class lasers. Journal of Engineering, 2015, 2015, 158-160.	1.1	1
238	Continuous-wave seeded mid-IR parametric system pumped by the high-average-power picosecond Yb:YAG thin-disk laser. Proceedings of SPIE, 2015, , .	0.8	1
239	Laser induced damage threshold of optical fibers under ns pulses. Proceedings of SPIE, 2016, , .	0.8	1
240	HiLASE: a scalable option for Laser Inertial Fusion Energy. Journal of Physics: Conference Series, 2016, 688, 012060.	0.4	1
241	Picosecond pulses in deep ultraviolet (257.5 nm and 206 nm) and mid-IR produced by a high-power 100 kHz solid-state thin-disk laser. Proceedings of SPIE, 2016, , .	0.8	1
242	A 100 J-level nanosecond DPSSL for high energy density experiments. Proceedings of SPIE, 2017, , .	0.8	1
243	Wavefront aberration measurement in a cryogenically cooled Yb:YAG slab using a wavefront sensor. , 2017, , .		1
244	Temperature dependent spectroscopic characterization of Tm:YAG crystals as potential laser medium for pulsed high energy laser amplifiers. , 2017, , .		1
245	Experimental Study of Nanosecond Laser-Generated Plasma Channels. Applied Sciences (Switzerland), 2020, 10, 4082.	2.5	1
246	Investigation of spectrally-dependent phonon relaxation mechanism in Yb:YAG gain media and its consequences for thin disk laser performance. Laser Physics, 2020, 30, 025005.	1.2	1
247	Silicon Brewster plate wavelength separator for a mid-IR optical parametric source. Applied Optics, 2021, 60, 281.	1.8	1
248	High Power Picosecond Parametric Mid-IR Source Tunable Between 1.5 and 3.2 l̂¼m. , 2018, , .		1
249	Highly Efficient Surface Modification of Solids by Dual Action of XUV/Vis-NIR Laser Pulses. Springer Proceedings in Physics, 2009, , 401-407.	0.2	1
250	Development of High Energy and High Average Power Ultrafast Thin Disk Lasers. The Review of Laser Engineering, 2013, 41, 703.	0.0	1
251	Influence of laser-beam focusing on the production of highly charged ions from laser plasma. , 1996, ,		1

A 100J-level nanosecond pulsed DPSSL., 2016, , .

#	Article	IF	CITATIONS
253	Laser beam distribution system for the HiLASE Center. , 2017, , .		1
254	High-Energy Burst Mode Thin-disk Multipass Amplifier for Laser Compton X-ray Source. , 2018, , .		1
255	100J-level nanosecond pulsed Yb:YAG cryo-cooled DPSSL amplifier. , 2018, , .		1
256	HILASE center: development of new-generation lasers for laser shock peening. , 2018, , .		1
257	Multiple pulse nanosecond laser-induced damage threshold on AR coated YAG crystals. , 2018, , .		1
258	Diode-pumped cryogenic Tm:LiYF4 laser. , 2019, , .		1
259	Shaping of picosecond laser pulses by second harmonic generation with time predelay. , 2020, , .		1
260	Lasing performance of crystalline-coated Yb:YAG thin disks. , 2021, , .		1
261	Analysis of broadband mid-infrared optical parametric amplification based on LiGaS <sub>2</sub> , LiGaSe <sub>2</sub> , LiInS <sub>2</sub> , and LiInSe <sub>2</sub> crystals. Journal of the Optical Society of America B: Optical Physics, 2022, 39, 1174.	2.1	1
262	Difference Frequency Generation in BaGa4Se7 Tunable in a 6.5-8.5 μm Range with a Peak Power of 30 MW Pumped by 1.03 μm, 1.8 ps Laser. , 2022, , .		1
263	Electron density profile measurements of line plasmas by interferometric technique. , 1996, 2767, 119.		Ο
264	Design of efficient soft X-ray laser using neonlike Fe driven by iodine laser. , 1996, , .		0
265	<title>X-ray laser progress for applications</title> ., 2001, 4505, 211.		Ο
266	<title>Soft x-ray emission from Ar clusters heated by ultrashort laser pulse</title> ., 2001, , .		0
267	<title>Intensity distribution of the focal lines of the prepulse and mainpulse at the solid target surface</title> . , 2001, 4424, 561.		0
268	Development and applications of X-ray lasers at LSAI/LIXAM. AIP Conference Proceedings, 2002, , .	0.4	0
269	Demonstration of lasing at 41.8 nm in Xe8+driven in a plasma waveguide. , 2003, , .		0
270	X-ray microscopy and imaging of Caenorhabditis elegans nematode using a laser-plasma-pulsed x-ray source. , 2004, , .		0

#	Article	IF	CITATIONS
271	<title>Laser-driven shock experiments at PALS</title> . , 2004, , .		0
272	<title>Carbon hugoniot at megabar pressures driven by laser-induced shocks</title> . , 2004, , .		0
273	Development and applications of 10-mJ x-ray lasers at PALS. , 2005, , .		0
274	Soft X-ray laser of second generation. , 2005, , .		0
275	Exposed sets in potential theoryâ~†â~†The work is part of the research project MSM 0021620839 financed by MSMT Bulletin Des Sciences Mathematiques, 2006, 130, 646-659.	1.0	0
276	Plasma Based X-ray Lasers Used For Opacity and Ablation Rate Measurements. AIP Conference Proceedings, 2006, , .	0.4	0
277	Development of ultrafast soft x-ray beamline at PALS and surface modification of solids by high-order harmonics. Proceedings of SPIE, 2007, 6702, 240.	0.8	0
278	Applications of a 10-mJ soft X-ray laser: from dense plasma physics to micro-structuring. , 2007, , .		0
279	Multidisciplinary Applications of Highly Energetic Soft X-Ray Laser at 21 nm. Conference Proceedings - Lasers and Electro-Optics Society Annual Meeting-LEOS, 2007, , .	0.0	Ο
280	21-nm x-ray laser Thomson scattering of laser-heated exploding foil plasmas. Proceedings of SPIE, 2007,	0.8	0
281	High-pressure behavior of carbon by laser-generated shocks. Russian Journal of Physical Chemistry A, 2007, 81, 1360-1364.	0.6	0
282	Development of ultrafast soft x-ray beamline based on high-order harmonic generation at PALS. , 2008, , .		0
283	Research on the seeding of high-energy harmonic pulse into an x-ray lasing medium. , 2009, , .		0
284	Applications of high energy X-ray lasers in plasma probing and warm dense matter generation. , 2009, , .		0
285	Efficient materials processing by dual action of XUV/Vis-NIR ultrashort laser pulses. , 2009, , .		0
286	Damage thresholds of various materials irradiated by 100-ps pulses of 21.2-nm laser radiation. , 2009, , .		0
287	Improved efficiency of materials processing by dual action of XUV/Vis-NIR ultrashort laser pulses and comprehensive study of high-order harmonic source at PALS. , 2009, , .		0
288	Preliminary studies on fast particle diagnostics for the future fs-laser facility at PALS. Radiation Effects and Defects in Solids, 2010, 165, 419-428.	1.2	0

#	Article	IF	CITATIONS
289	Advances in laser driven soft x-ray lasers at LOA. Proceedings of SPIE, 2011, , .	0.8	Ο
290	Numerical evaluation of heat deposition in cryogenically cooled multi-slab amplifier. Proceedings of SPIE, 2011, , .	0.8	0
291	Efficient surface processing by ultrafast XUV/NIR dual action. , 2011, , .		0
292	100-J level amplifier concepts for HiLASE and ELI-Beamlines. , 2012, , .		0
293	High-energy regenerative thin disk amplifier. , 2012, , .		0
294	30-mJ, 1-kHz, Yb:YAG thin disk regenerative amplifier with pulsed pumping at 969-nm. , 2013, , .		0
295	1-kHz pulsed pumped Yb:YAG thin disk regenerative amplifier. , 2013, , .		0
296	Modeling and optimization of thin disk structure for high power sub-joule laser. , 2013, , .		0
297	Advantages of zero phonon line pumping in 100kHz Yb:YAG thin-disk regenerative amplifier. , 2013, , .		0
298	Design of a tunable parametric wavelength conversion system between 2 and 3 μm pumped by a high-average-power Yb:YAG thin-disk laser. , 2013, , .		0
299	Effective mid-IR pulse generation pumped by high average power thin disk regenerative amplifier. , 2013, , .		0
300	Simple measurement of picosecond laser pulses in a wavelength range above $1^{1/4}$ m. , 2013, , .		0
301	Design of kJ-class HiLASE laser as a driver for inertial fusion energy – CORRIGENDUM. High Power Laser Science and Engineering, 2014, 2, .	4.6	0
302	EUV ablation of organic polymers at a high fluence. High Power Laser Science and Engineering, 2014, 2,	4.6	0
303	Cryogenic laser performance of Yb:YAG diode-pumped at 940 nm and 969 nm for high power lasers. , 2014, , .		0
304	Design and optimization of an adaptive optics system for a high-average-power multi-slab laser (HiLASE): erratum. Applied Optics, 2014, 53, 7877.	2.1	0
305	Development of short pulse CO2 laser for efficient rare earth plasma extreme ultraviolet sources. , 2015, , .		0
306	Laser fluence dependence of periodic structures on metals produced by femtosecond double pulse laser. , 2015, , .		0

#	Article	IF	CITATIONS
307	Experimental benchmarking of the code for Yb:YAG multi-slab gas-cooled laser system operating at cryogenic temperatures. , 2015, , .		Ο
308	Picosesond pulses in deep ultraviolet produced by a 100 kHz solid-state thin disk laser. Proceedings of SPIE, 2015, , .	0.8	0
309	Joule-class 940 nm diode laser bars for millisecond pulse applications. , 2015, , .		Ο
310	First experimental test of quadrupole lens-free multiple profile monitor technique for electron beam emittance measurement with a PW laser system. Proceedings of SPIE, 2015, , .	0.8	0
311	Single shot M <sup>2</sup> measurement for near infrared high energy laser pulses. Proceedings of SPIE, 2015, , .	0.8	Ο
312	Assessment of high-power kW-class single-diode bars for use in highly efficient pulsed solid state laser systems. , 2015, , .		0
313	Timing jitter measurement and stabilization of a mode-locked ytterbium fiber laser. Proceedings of SPIE, 2015, , .	0.8	Ο
314	Focal spot of femtosecond laser pulse under tight focusing condition. Proceedings of SPIE, 2015, , .	0.8	0
315	Experimental and theoretical study of deformable mirror actuator arrays. Proceedings of SPIE, 2015, , .	0.8	Ο
316	HiLASE Project: high intensity lasers for industrial and scientific applications. , 2015, , .		0
317	Tunable diode laser absorption spectroscopy on 2.05 μm for the CO <sub>2</sub> concentration measurement. Proceedings of SPIE, 2015, , .	0.8	Ο
318	Formation of laser induced periodic surface structures (LIPSS) on Ti upon double fs pulse exposure. , 2015, , .		0
319	Development of a closed-loop cryogenically cooled sub-picosecond regenerative amplifier. , 2015, , .		0
320	Recent Advances on the J-KAREN laser upgrade. , 2015, , .		0
321	Innovative opto-mechanical design of a laser head for compact thin-disk. Proceedings of SPIE, 2016, , .	0.8	0
322	Development of a kW-level picosecond thin-disk regenerative amplifier with a ring cavity. , 2016, , .		0
323	Zero-phonon-line pumped cryogenic Yb:YAG passively Q-switched by Cr:YAG. Proceedings of SPIE, 2016, , .	0.8	0
324	Cryogenically-cooled Yb:YGAG ceramic picosecond oscillator. Proceedings of SPIE, 2016, , .	0.8	0

#	Article	IF	CITATIONS
325	Investigation and modelling of pump saturation effect on thermal load of Yb:YAG thin disk pumped at various wavelengths. Proceedings of SPIE, 2017, , .	0.8	0
326	Development of 2.7-μm Er:Y2O <sub>3</sub> ceramic laser operated at room temperature. Proceedings of SPIE, 2017, , .	0.8	0
327	Demonstration of laser oscillation of an Yb-doped Y <inf>2</inf> O <inf>3</inf> composite disk by use of atomic diffusion bonding in room temperature. , 2017, , .		0
328	The first kilowatt average power 100J-level DPSSL. , 2017, , .		0
329	HiLASE: New lasers for industry and research. , 2017, , .		0
330	Cryogenic Yb:YGAG ceramic laser pumped at 940 nm and zero-phonon-line: a comparative study. Optical Materials Express, 2017, 7, 477.	3.0	0
331	kW-class picosecond and nanosecond lasers at Hilase for hi-tech industrial applications. , 2017, , .		0
332	The first multi-joule DPSSL with 1 kW average power. , 2017, , .		0
333	Single Shot M2 Measurement for Near Infrared Laser Pulses in Real-Time. , 2019, , .		0
334	Picosecond Deep Ultraviolet Pulses Generated in Excess of the 1030 nm Fundamental Beam. , 2019, , .		0
335	Characterization of the Verdet Constant of Dy2O3 Ceramics in the Two-Micron Spectral Range. , 2019, , $\cdot$		0
336	Peak Power Enhancement of Yb:YAG Laser Pulses by Second Harmonic Generation with Time Predelay in Borate Crystals. , 2019, , .		0
337	Dependencies of Picosecond Pulse Driven Supercontinuum Properties on Repetition Rate. , 2019, , .		0
338	Diode — Pumped Efficient Cryogenic Yb:Y2O3 Transparent Ceramic Laser. , 2019, , .		0
339	Spectroscopy, Continuous-Wave and Passively Q-Switched Laser Operation of Transparent Tm:LuAG Ceramics. , 2019, , .		0
340	Spectroscopy of Tm:Y2O3 Transparent Ceramic at Cryogenic Temperatures. , 2019, , .		0
341	Development of a High-Quality Epoxy Bonding Technology. , 2019, , .		0
342	Laser Annealing of Anodic TiO2 Nanotubes: Explosive Solid Phase Crystallization into Anatase. , 2021, , .		0

#	Article	IF	CITATIONS
343	Picosecond VIS, UV and Deep UV Beams Generated at 100 kHz Diode-Pumped Yb:YAG Thin Disk Laser System. , 2021, , .		0
344	2 μm MOPA Laser Based on Cryogenically Cooled Tm:Y2O3 Transparent Ceramic. , 2021, , .		0
345	Investigations on femtosecond-pulse-driven soft X-ray lasers using a gas puff target irradiated with a Ti:Sapphire laser. European Physical Journal Special Topics, 2001, 11, Pr2-197-Pr2-200.	0.2	0
346	Intensity distribution of the focal lines of the prepulse and mainpulse at the solid target surface. European Physical Journal Special Topics, 2001, 11, Pr2-601-Pr2-604.	0.2	0
347	Interaction of intense, femtosecond laser pulse with small-sized Ne clusters. European Physical Journal Special Topics, 2001, 11, Pr2-433-Pr2-436.	0.2	0
348	Lasers XUV collisionnels pompés par des lasers femtoseconde. European Physical Journal Special Topics, 2003, 108, 161-164.	0.2	0
349	Lasers collisionnels à 41.8 nm en régime guidé. European Physical Journal Special Topics, 2005, 127, 33-37.	0.2	0
350	Lasers X de deuxième génération. European Physical Journal Special Topics, 2005, 127, 9-13.	0.2	0
351	Laser X-UV en schéma collisionnel OFI à 41,8 nm créé dans des tubes capillaires. European Physical Journal Special Topics, 2006, 138, 43-53.	0.2	0
352	Microscopie interférentielle X-UVÂ: un outil pour l'étude des endommagements des surfaces optiques. European Physical Journal Special Topics, 2006, 138, 245-250.	0.2	0
353	Innershell X-Ray Laser in Sodium Vapor: Final Steps Towards Experimental Verification. Springer Proceedings in Physics, 2009, , 557-562.	0.2	0
354	Characterization of a seeded optical-field ionized collisional soft x-ray laser. Springer Proceedings in Physics, 2011, , 127-135.	0.2	0
355	HiLASE: Development of Fully Diode-Pumped, kW-Class Pulsed Lasers for High-Tech Applications. The Review of Laser Engineering, 2014, 42, 145.	0.0	0
356	Development of the estimation method for thermo-optics effects in the TGG ceramics rod. , 2014, , .		0
357	Microchip Laser Operation of Yb-Doped Gallium Garnets. , 2015, , .		0
358	Parametric Mid-IR Source Pumped by a High Power Picosecond Thin-Disk Laser. , 2016, , .		0
359	Wavelength Tunable Picosecond Parametric Mid-IR Source Pumped by a High Power Thin-Disk Laser. , 2017, , .		0
360	Diode-pumped femtosecond Yb:YGAG regenerative amplifier. , 2017, , .		0

21

#	Article	IF	CITATIONS
361	Wavelength tunable parametric mid-IR source pumped by a high power picosecond thin-disk laser. , 2017, , .		0
362	A practical model of thin disk regenerative amplifier based on analytical expression of ASE lifetime. , 2017, , .		0
363	Large Scale Single Crystal Growth. , 2018, , .		Ο
364	A Femtosecond 8.5 $\hat{l}$ $\!\!\!\!/4$ m Source Based on Intrapulse Difference-Frequency Generation of 2.1 $\hat{l}$ $\!\!\!\!/4$ m Pulses. , 2018, , .		0
365	Development of experimental station for laser shock peening at HiLASE. , 2018, , .		Ο
366	Ten-watt level picosecond parametric mid-IR source broadly tunable in wavelength. , 2018, , .		0
367	Generation of 1-J bursts with picosecond pulses from Perla B thin-disk laser system. , 2018, , .		Ο
368	Wavefront correction with photo-controlled deformable mirror. , 2018, , .		0
369	High-energy subpicosecond 2.1-um fiber laser. , 2018, , .		0
370	Laser induced damage in optical glasses using nanosecond pulses at 1030 nm. , 2018, , .		0
371	Synthesis, Spectroscopy and Efficient Laser Operation of Tm:Lu3Al5O12 Transparent Ceramics. , 2019, , .		0
372	Concepts for Adapting Highly Efficient Diode Pumped Laser Technology for Laser Shock Peening. , 2019, , .		0
373	Thermo-optical Study of 10 J/ 100 Hz Cryogenically Cooled Yb:YAG Diode Pumped Laser System. , 2019, , .		Ο
374	Importance of Laser Induced Damage Threshold for Laser Applications. , 2019, , .		0
375	Highly efficient, cryogenically cooled Yb:YAG q-switch laser based on a gain modulated unstable resonator design. , 2019, , .		Ο
376	Monocrystalline materials for high-power ultrafast lasers. , 2019, , .		0
377	Single-shot laser beam parameter measurement system for near-infrared laser beams. Journal of the Optical Society of America B: Optical Physics, 2019, 36, 3098.	2.1	0
378	Comparison of multipulse nanosecond LIDT of HR coated YAG and glass substrates at 1030 nm. , 2019, , .		0

#	Article	IF	CITATIONS
379	Mobile LIDT. , 2019, , .		Ο
380	Modular laser beam distribution system for the HiLASE Center. , 2019, , .		0
381	EUV SOURCE AT HILASE: THE STATE OF THE ART. MM Science Journal, 2019, 2019, 3406-3409.	0.4	0
382	Multi-watt continuous-wave and passively Q-switched Tm:CaYAlO4 micro-lasers. , 2020, , .		0
383	Multiple pulse picosecond laser induced damage threshold on hybrid mirrors. , 2020, , .		0
384	Influence of the CVBG compressor on output parameters of high-power and high-energy laser beam. , 2021, , .		0
385	Spectral broadening and a prospect for pulse compression of Yb:YAG thin-disk laser pulses by nonlinear SHG in a BBO crystal with time predelay and tilting of the pulse fronts. , 2022, 1, 16.		0
386	Qualification of 1030 nm ultra-short-pulsed laser for glass sheet treatment in TGV process. , 2022, , .		0